

Optimal distribution for photovoltaic solar trackers to minimize power losses caused by shadows

Eloy Díaz-Dorado, Andrés Suárez-García*, Camilo J. Carrillo, José Cidrás

E.T.S. de Enxeñeiros Industriais de Vigo, Enxeñería Eléctrica, Campus Universitario, 3610 Vigo, Pontevedra, Spain

ARTICLE INFO

Article history:

Received 27 September 2010

Accepted 2 December 2010

Available online 31 December 2010

Keywords:

Evolutionary computation

Photovoltaic Systems

ABSTRACT

The typical design of photovoltaic facilities with photovoltaic solar trackers is achieved using a squared or diagonal distribution of the trackers. In general, this is a good distribution for harvesting most solar radiation. However, these facilities can be affected by shadows of environmental objects like buildings, vegetation, etc. In this paper, a metaheuristic method based on evolution strategies is presented for calculating the best location of each tracker on a building of irregular shape, considering the shadows caused by obstacles and photovoltaic trackers. The evolution strategies will use the energy readings obtained by a photovoltaic tracker distribution to look for the best location. In the calculus of the energy, solar charts are used to combine the solar radiation received and shadows suffered by the tracker for each solar position.

© 2010 Elsevier Ltd. All rights reserved.

1. Introduction

The best way of obtaining the maximum power from the photovoltaic arrays (PV arrays) is to add a tracking mechanism, thus ensuring sunlight is always perpendicular to the surface of the photovoltaic cells (PV cells). The photovoltaic solar trackers (PV trackers) can collect up to 40% more solar radiation than static PV arrays, thus more electrical energy is generated.

A single computing model is presented in this paper in order to decide the best two-axis PV tracker distribution in the field, taking into account the shadow losses. Several authors only consider static PV arrays [1–8]. In these cases, PV modules must be mounted with correct direction and angle to get the maximum solar radiation [1,2]. Different models have been developed to analyze the influence shadows have on the electrical energy produced by the PV arrays [9–14]. An examination has also been made to determine which is the best connection setting between solar cells [12,13,15,16].

In large photovoltaic fields (PV fields) the typical distribution of PV arrays is in squares or diagonals [1]. However, in PV fields of a small and medium size, the parcel geometry and the environment obstacles demand a non-symmetric distribution of the PV systems, in order to achieve the maximum efficiency of the PV installation.

This article proposes a heuristic method [17] to determine the optimal distribution of a PV tracker, taking into consideration the energy losses caused by shadows from other PV trackers, walls, the horizon, etc. The following sections will explain the different parts of the method. Section 2 shows the solar chart of direct and diffuse solar radiations and how to measure them. Section 3 describes how to calculate the shadow suffered by a PV tracker for all solar positions. Section 4 points out how to calculate the electrical energy obtained by a PV tracker, taking into account the shadow projected onto it. Section 5 explains the heuristic strategy used to determine the optimal distribution of the PV trackers in a PV field, using the electrical energy of the PV field as the criteria for achieving the optimal distribution. Section 6 details the examples of calculus obtained from the method described in Section 5. Finally, conclusions are presented in Section 7.

2. Cylindrical solar energy chart

Solar positioning can be pinpointed using cylindrical coordinates: the solar position azimuth α and elevation γ (Fig. 1). In this article, the reference of the azimuths is North ($\alpha_{NORTH} = 0^\circ$), the rest of the azimuths are measured in the clockwise sense ($\alpha_{EAST} = 90^\circ$, $\alpha_{SOUTH} = 180^\circ$ and $\alpha_{WEST} = 270^\circ$).

The amount of solar radiation received by a PV tracker depends on the solar position. The cylindrical solar energy chart (Fig. 2) is the representation of the energy received in relation to the solar position. The data needed to plot a chart can be obtained either from a meteorological station or can be calculated by using celestial

* Corresponding author. Tel.: +34 986 813912; fax: +34 986 812173.
E-mail address: ansuga@uvigo.es (A. Suárez-García).

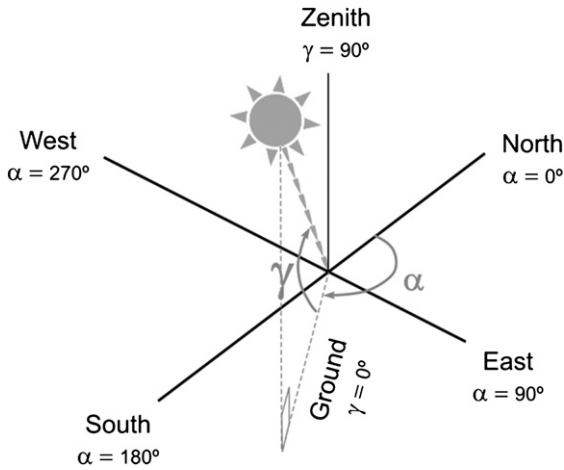


Fig. 1. Sun position defined by its azimuth (α) and elevation (γ).

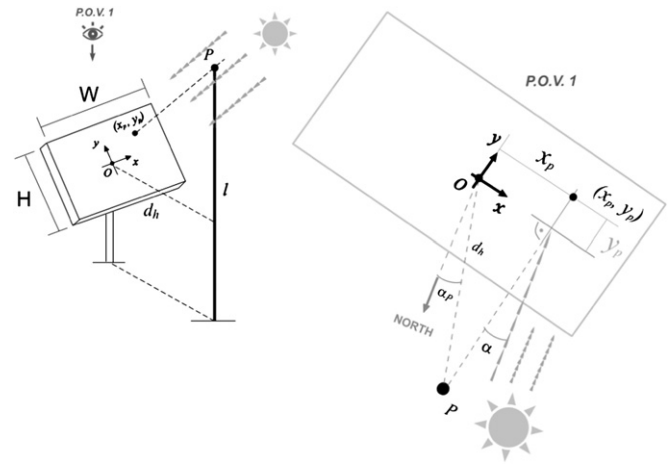


Fig. 3. Calculus of the shadow projected by a point (coordinate x_p).

mechanics [18]. In Fig. 2, direct and diffuse energy is represented. These values were obtained using data from Monte Aloia meteorological station (<http://www.meteogalicia.es>).

Only a fraction of the solar radiation gets to the surface of the PV tracker. In the PV field there are objects that are in the trajectory of the sun's rays, which absorbs part of the solar radiation. Because of that, the shadows appear on the PV tracker. Therefore, the calculus of the shaded surface is needed to know the solar radiation that receives a PV tracker.

3. Shadows

The objects in a PV tracker field can be modelled as: solar tracker planes (PV trackers) and static planes (posts, obstacles, building walls...). This section uses a fast algorithm to determine the shadow cast by these objects. For the sake of simplicity, cases will be explained in the following order:

- A. Shadow cast by a point.
- B. Shadow cast by a solar tracker plane.
- C. Shadow cast by a static plane.

In the calculus of all the cases, the shaded PV tracker centre is the origin of coordinates. In other words, the centre of the shaded PV tracker is the observer in the solar chart, and for each solar azimuth and elevation, the total amount of received radiation is calculated taking into account the percentage of the shaded PV tracker. For simplicity, the centre and the pivot point of the PV tracker has been supposed as the same point. If there was a need to take into account the difference between both points, it could be easily found and used through vectorial calculus.

3.1. Shadow cast by a point

The shadow cast by a point P on a PV tracker of width W and height H facing the Sun, is represented by the coordinates (x_p, y_p) . The coordinate x_p only depends on the solar azimuth (Fig. 3), whereas the coordinate y_p also depends on the solar elevation (Fig. 4).

$$x_p = d_h \cdot \sin(\alpha_p - \alpha) \tag{1}$$

where:

- d_h is the distance between the PV tracker centre O and the point P projected in an horizontal plane.
- α_p is the P azimuth.
- α is the solar azimuth.

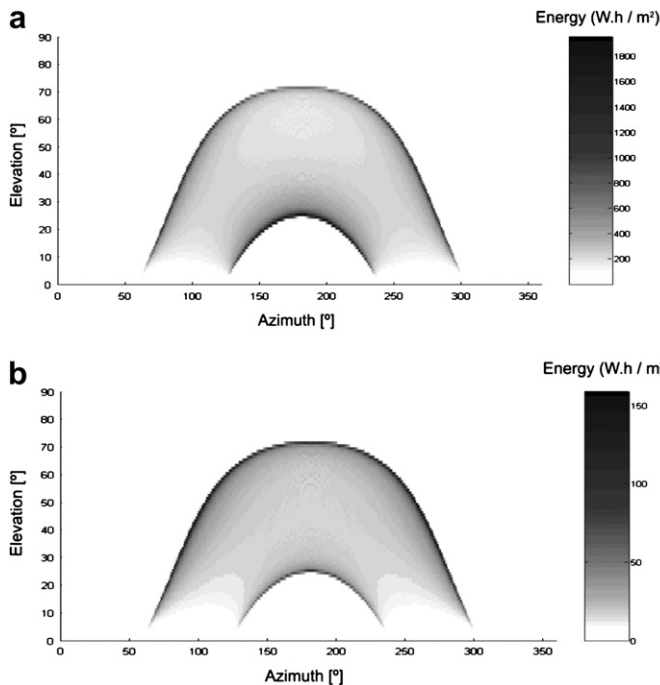


Fig. 2. Cylindrical solar chart of solar energy (a) direct (b) diffuse ($W.h/m^2$).

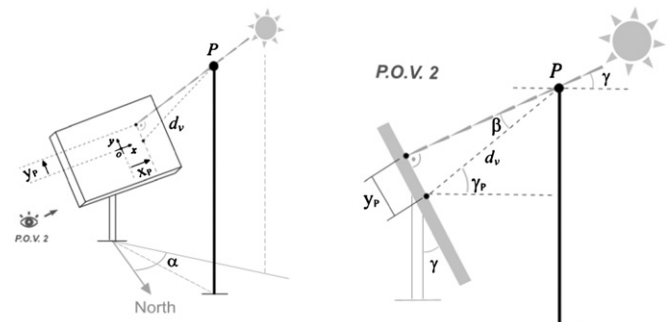


Fig. 4. Calculus of the shadow projected by a point (coordinate y_p).

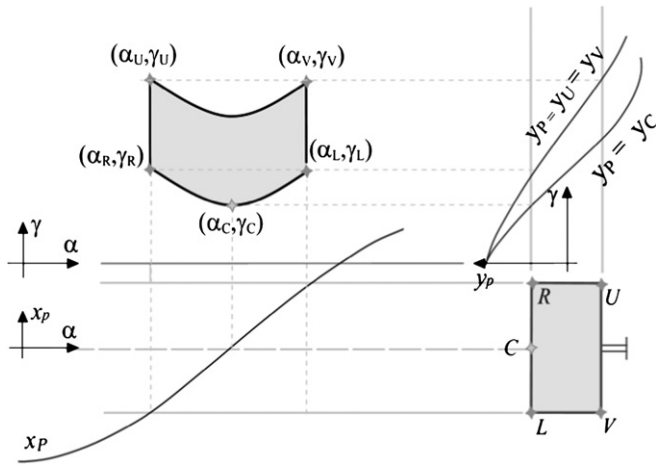


Fig. 5. Solar chart of the point shading on a PV tracker.

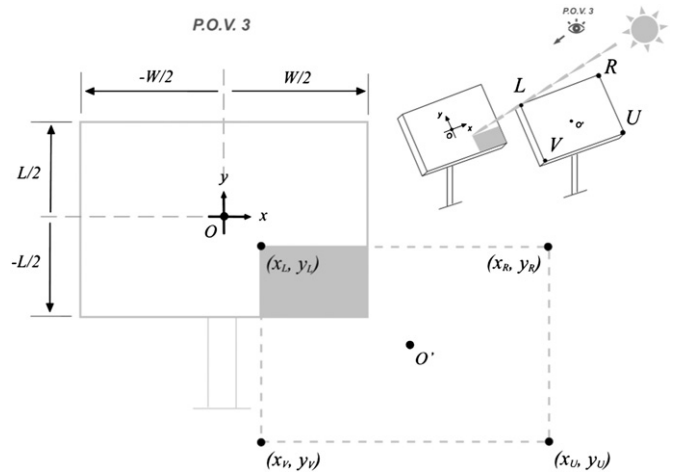


Fig. 7. Shadow projected by another PV tracker.

$$y_p = d_v \sin(\gamma_p - \gamma) \tag{2}$$

where:

- d_v is the distance between (x_p) and the point P .
- γ_p is the P elevation.
- γ is the solar elevation.

A shadow chart can be obtained representing the solar positions where the point P projects its shadow on the PV tracker (Fig. 5). There are three zones in Fig. 5. The central zone represents the solar positions where point P casts its shadow on the PV tracker. In the lower part, it shows x_p in relation to the solar azimuth, α . In the right zone, it shows y_p in relation to the solar elevation, γ , for different values of x_p . The points (α_R, γ_R) , (α_L, γ_L) , (α_U, γ_U) and (α_V, γ_V) are the solar positions where the shadow of point P is projected on the PV tracker corners, R, L, U and V .

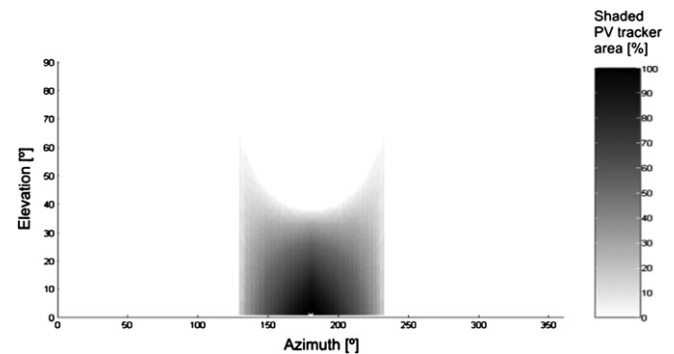


Fig. 8. Percentage of shaded area caused by a close PV tracker.

- i. The curves of the solar chart are exaggerated for explanatory purposes. There is a distortion of the rectangle due to the use of polar coordinates in the solar chart. However, the superior curvature is hardly noticeable except in cases where point P is near to the PV tracker.
- ii. The inferior corners of the shaded PV tracker, U and V , have equal y_p because their distance d_v is equal. The same can be said of the superior corners R and L .
- iii. The points (α_U, γ_U) and (α_V, γ_V) are respectively above the points (α_R, γ_R) and (α_L, γ_L) , because a greater solar elevation is needed for the line shadow to reach them (Fig. 6).

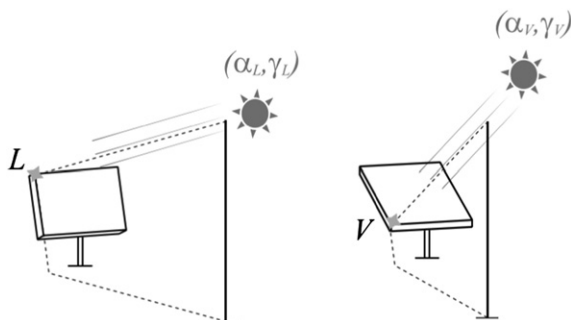


Fig. 6. Shadow of a point over the corners of a PV tracker.

3.2. Shadows caused by a PV tracker on another PV tracker

The shadow cast by a PV tracker on another PV tracker is defined by the projection of the corners of the first one (R, L, U and V) over the second one, and the limits of the shaded one (Fig. 7).

A shadow map for each solar azimuth and elevation can be created using the percentage of shaded area (Fig. 8). The incoming radiation is obtained multiplying the shaded area in v.p.u. for the solar radiation in each solar azimuth and elevation.

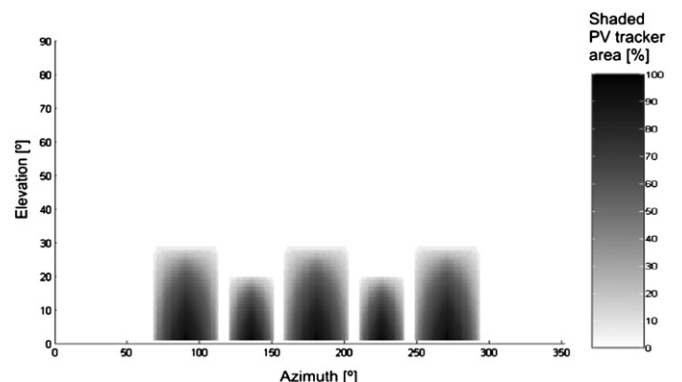


Fig. 9. Percentage of shaded area caused by five distant PV trackers.

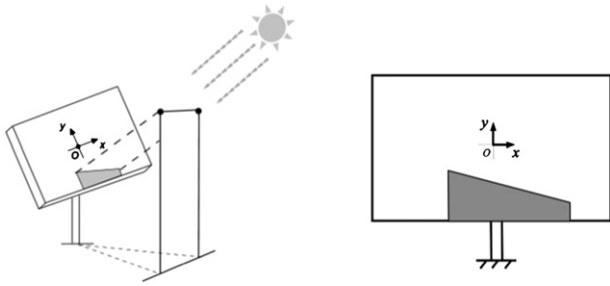


Fig. 10. Shadow cast by a vertical plane.

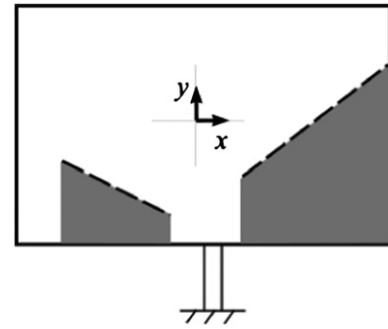


Fig. 12. Non-overlapped shadows.

If there are various PV trackers with non-overlapped shadows, the algorithm of calculus is the same for each one of them (Fig. 9). But if there is overlapping between shadows, the algorithm must be modified to avoid counting twice the overlapped shadows, as will be explained later.

3.3. Shadow cast by a vertical plane on PV tracker

The calculus is similar to that which has just been explained in Section 3.2. Only the four corners of the plane are needed for this calculus. It must be emphasized that this simplification can only be made with vertical planes, because all the points in the vertical edges have equal horizontal distance, d_h in expression (1), to the centre of the PV tracker. Therefore, the shadow will have its lateral edges perpendicular to the PV tracker bottom (Fig. 10).

Fig. 11 has been created by plotting the percentage of shaded PV tracker area in relation to the solar azimuth and elevation.

3.4. Superposition of shadows

To measure the area shaded by two objects, it cannot be done separately and then be added together, because the shadow would be added twice in the common shaded areas. To avoid counting the same shadow twice, there are two methods of calculus, depending on the existence of overlapped shadows.

If the shadows don't overlap, they are calculated separately and then add them together (Fig. 12).

However, if they cross themselves, the calculus is done in separate intervals, obtaining for each interval its shadow area. The different intervals of the shadow calculus are defined by the crossing point $P_c(x_c, y_c)$. This point can be calculated because the points L_1, L_2, R_1 and R_2 are known (Fig. 13).

In this section it has been explained how to work out the total shaded area of two overlapped shadows. A result of this calculus

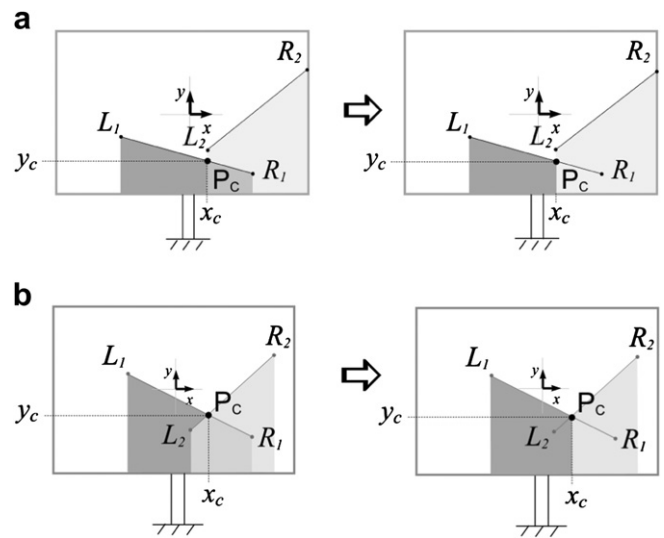


Fig. 13. Sum of overlapped shadows with (a) non-crossing superior edges (b) crossing superior edges.

can be seen in Fig. 14. The overlap of a greater number of shadows is progressively done taking the shadows in pairs.

3.5. Energy reduction produced by shadows

Once the percentage of shadow for a solar azimuth α and solar elevation γ is calculated (Fig. 11), it is then subtracted from the solar

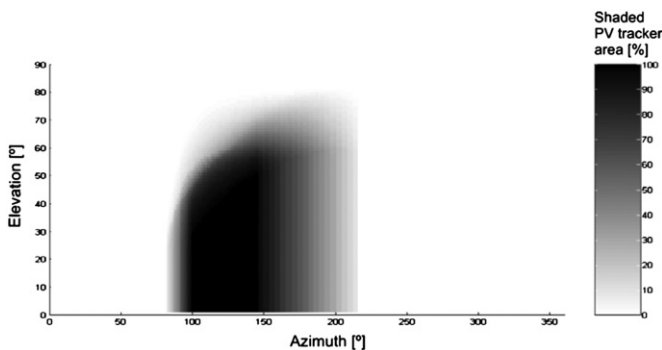


Fig. 11. Percentage of shaded PV tracker area produced by a vertical plane.

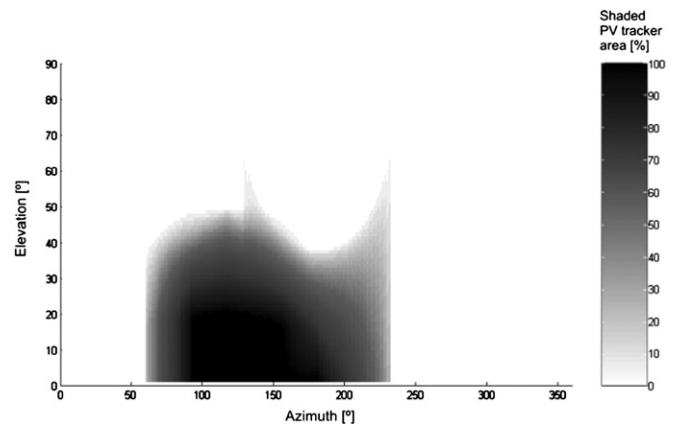


Fig. 14. Sum of overlapped shadows of a vertical plane and a PV tracker.

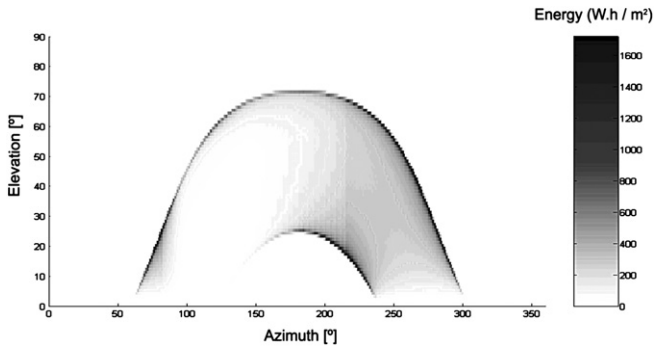


Fig. 15. Solar energy chart taking into account the shadow of a vertical plane.

energy obtained for the same α and γ (Fig. 2(a)) in order to obtain the radiation received by the PV tracker (Fig. 15). This process is only done for the solar direct radiation, because the amount of the solar diffuse radiation received by the PV tracker is not affected by shadows.

As it can be seen, the calculus of the shadows projected on a PV tracker is important in order to know the amount of solar energy received by the surface of the PV tracker. This solar radiation will be transformed into electrical energy.

4. Electrical energy

Each PV tracker is formed by an array of photovoltaic modules. Each PV module is a set of PV cells with bypass diodes connected in parallel. Bypass diodes are parallel connected to a group of PV cells to enable an alternative path for electrical flow in cases where a number of PV cells of the group could consume energy. This could happen if they were shaded, covered, or damaged (Fig. 16).

The bypass diodes modify the curve I–V of the PV tracker in relation to the PV cells shaded (Fig. 17). So, the electrical power obtained will depend on the diode configuration [19,20]. To achieve the highest performance, the control systems of the inverters will always seek the MPP. To ensure it is working at the optimum point, the inverter changes the working voltage in small amounts and compares the power of the actual working point with its nearest points. If it finds a point with greater power, that will become the new working point. When the PV modules are shaded, the problem of the inverter is that the global optimum point can possibly be too far away from the working point so that the inverter cannot reach it. Consequently, the point reached by the inverter can then be a local optimum point.

An extreme case is where the shadow is produced in cells of different series connected in parallel. In this case the working point

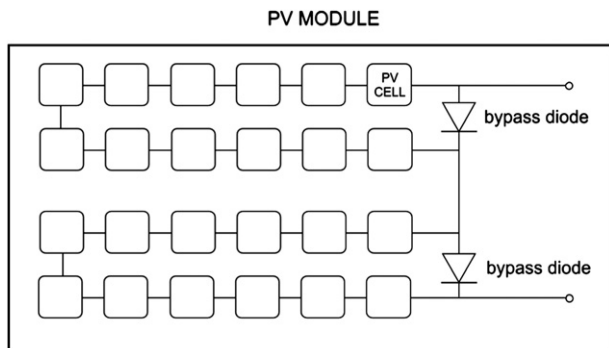


Fig. 16. PV modules with 2 bypass diodes and 1 blocking diode.

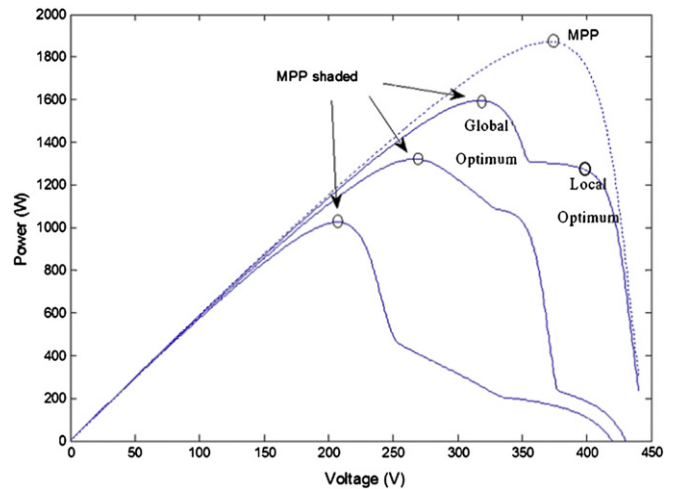


Fig. 17. Example of I–V curve of a PV tracker affected by shadows.

decreases rapidly, while the global optimum only varies a little (Fig. 18).

These effects on its efficiency will be simplified using a curve (Fig. 19) with maximum, minimum and average value of the electrical power obtained for the possible combinations of shaded solar cells. For an in-depth study see Ref. [21].

The electrical energy obtained in a PV tracker is essential in order to know how much energy is produced by a PV field. This fact is important to recognize the best PV tracker layout amongst all of possible layouts, and it will be employed in the metaheuristic algorithm as its function cost.

5. Evolution strategy

The method introduced in this paper is a heuristic process to establish the optimal location of PV solar trackers with two axes. The selected heuristic process is an evolutionary strategy algorithm of type $ES(\mu + \lambda)$ [17]. The principal advantage of this approach is that there is no need to solve the non-linear equations of the problem. Other advantage of genetic algorithms is that they can be modified to optimize more parameters, like the number of PV trackers, connections between solar cells, etc. Therefore, there are many possibilities to obtain better performances in the PV fields using these kinds of algorithms.

The following paragraphs describe the parts of the proposed algorithm (Fig. 20): population codification, crossover, mutation, selection operators and cost function.

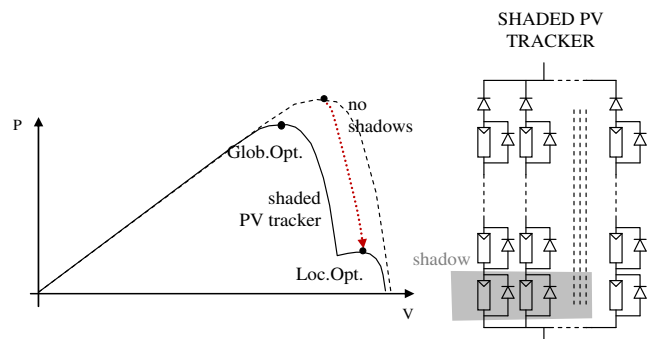


Fig. 18. Extreme case of shadow effects in the MPP tracking algorithm.

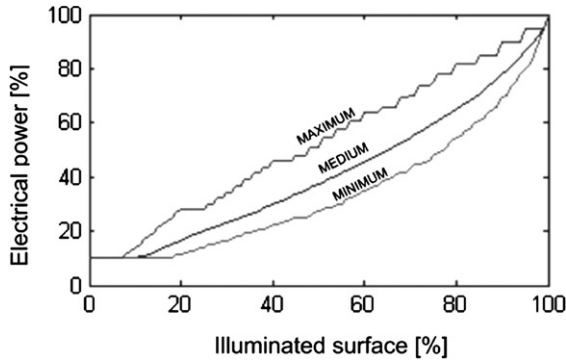


Fig. 19. Electrical power in relation to illuminated surface (non-shaded surface) for a diffuse radiation of 10%.

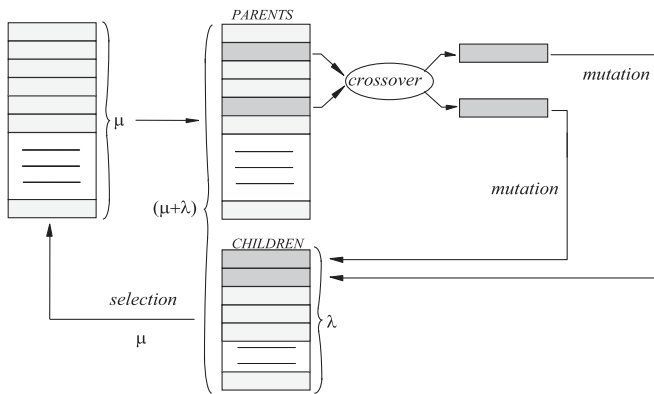


Fig. 20. Parts of an evolution strategy.

5.1. Population codification

The process begins with a group of random solutions. Each one is a possible layout for the PV trackers in the PV field. The group of solutions will be modified in an iterative way to find out which one is the best, by means of mutation and crossover operators. This group of solutions is the population of our evolution strategy. For the codification of a solution (Fig. 21) U.T.M. coordinates of the PV tracker centre have been used.

Also, a parameter is needed for each coordinate in order to define the mutation (see Section 5.2). A standard deviation σ of each coordinate is the mutation operator. Thus, the position of each PV tracker and its standard deviation are needed for the codification of a solution (Fig. 22).

5.2. Mutation and crossover operators

The mutation and crossover operators are the mechanisms employed to modify the population in the evolution strategies.

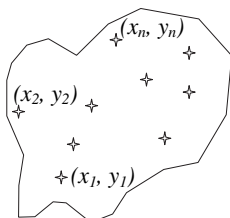


Fig. 21. PV trackers layout.

$$\begin{pmatrix} \vec{x}_k, \vec{y}_k \\ \vec{\sigma}_{x_k}, \vec{\sigma}_{y_k} \end{pmatrix} \begin{matrix} x_1 & y_1 & x_2 & y_2 & \dots & \dots & x_n & y_n \\ \sigma_{x1} & \sigma_{y1} & \sigma_{x2} & \sigma_{y2} & \dots & \dots & \sigma_{xn} & \sigma_{yn} \end{matrix}$$

Fig. 22. PV trackers layout codification.

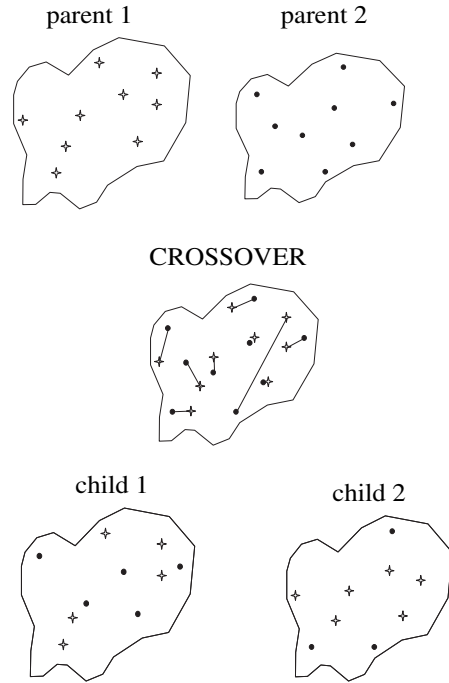


Fig. 23. Crossover.

These mechanisms guarantee new characteristics (mutation operator) and combined ones (crossover operator) in each of the successive generations.

5.2.1. Mutation operator

In evolution strategies the mutation operator is built using a Normal distribution $N(0, \sigma)$, associated to each coordinate.

$$\begin{matrix} x_i^{(t)} = x_i^{(t-1)} + v_{x_i} & v_{x_i} \sim N(0, \sigma_{x_i}^{(t)}) \\ y_i^{(t)} = y_i^{(t-1)} + v_{y_i} & v_{y_i} \sim N(0, \sigma_{y_i}^{(t)}) \end{matrix} \quad (3)$$

The standards deviations σ_x and σ_y are associated to each coordinate x and y . These deviations are also modified in each iteration, and they are defined by the expression:

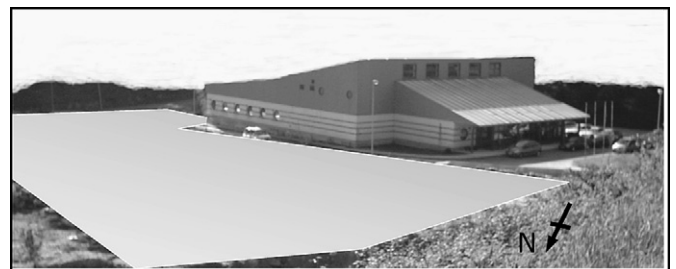


Fig. 24. Example of the plot with a house 41°54'N, 8°52'W.

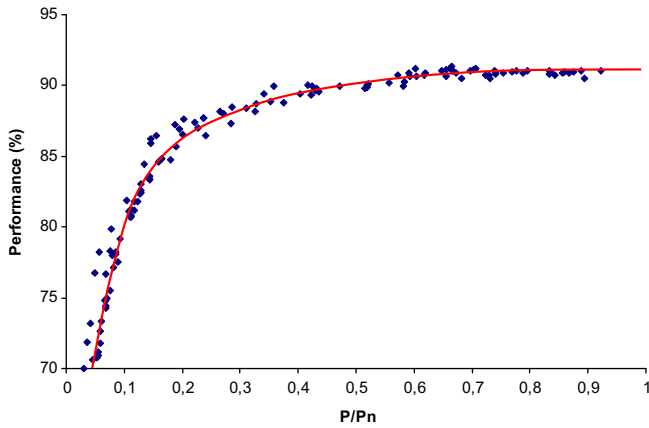


Fig. 25. Efficiency of the inverter.

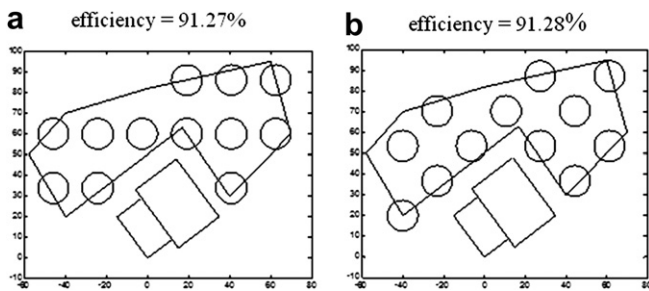


Fig. 26. PV trackers distribution using classical configurations (a) square (b) diagonal.

$$\begin{aligned} \sigma_{x_i}^{(t)} &= \sigma_{x_i}^{(t-1)} \cdot e^{(z_0 + z_i)} \\ \sigma_{y_i}^{(t)} &= \sigma_{y_i}^{(t-1)} \cdot e^{(z_0 + z_i)} \end{aligned} \quad (4)$$

where:

t is the number of the iteration.

z_0 is a random Normal variable with zero mean and a constant standard deviation τ_0 . z_0 is different for each solution of the same generation.

z_i is a random Normal variable with zero mean and a constant standard deviation τ_i . z_i is different for each coordinate of the same solution.

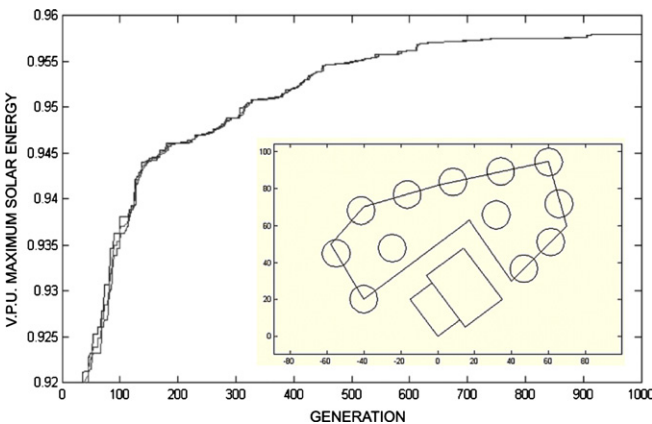


Fig. 27. Evolution of the PV solution efficiency in the plot with a house, and final solution.

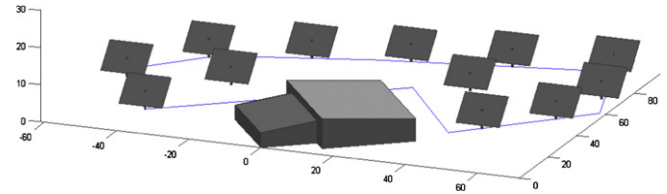


Fig. 28. Best location of the 12 PV trackers in the plot with a house.

$$z_0 \sim N(0, \tau_0) \quad z_i \sim N(0, \tau_i) \quad (5)$$

5.2.2. Crossover operator

The crossover operator is applied to two solutions (parents) for obtaining two new solutions (children) with mixed characteristics of both parents (Fig. 23). The steps to follow are:

- 1) Random selection of 2 parents among all the population members.
- 2) For each chromosome (coordinates x_i, y_i) of one parent, it will be assigned a couple chromosome of another parent by proximity priority.
- 3) Two children will be generated. For each one, components of the paired chromosomes will be randomly assigned without repetition.

5.3. Selection operator

When the mutation and crossover operators are finished, the population will be of size $\mu + \lambda$, where μ is the number of parents and λ is the number of children. A selection process is required to return the population to size μ . The selection operator consists in choosing μ members of among the best $\mu + \lambda$ members according to a cost function (survival function). This cost function will be described in the next section.

5.4. Cost function

The cost function is defined by the optimization problem. The objective of the present work is to maximize the total electric energy obtained by the PV trackers of the PV facility during a mean year. Thus, the cost function of each population member (or

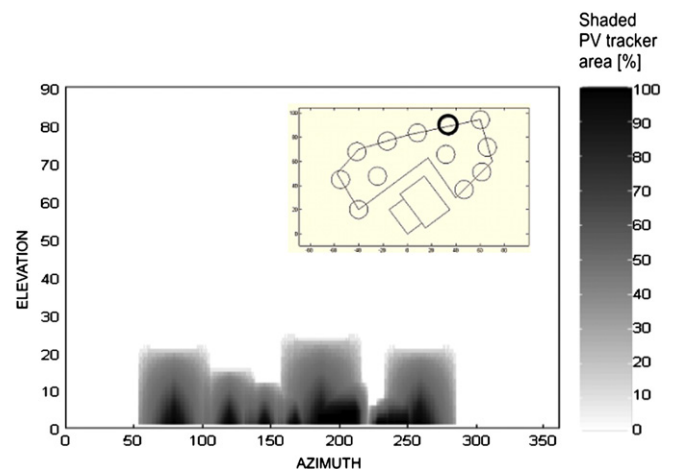


Fig. 29. Tracker affected by shadows shown in bold.

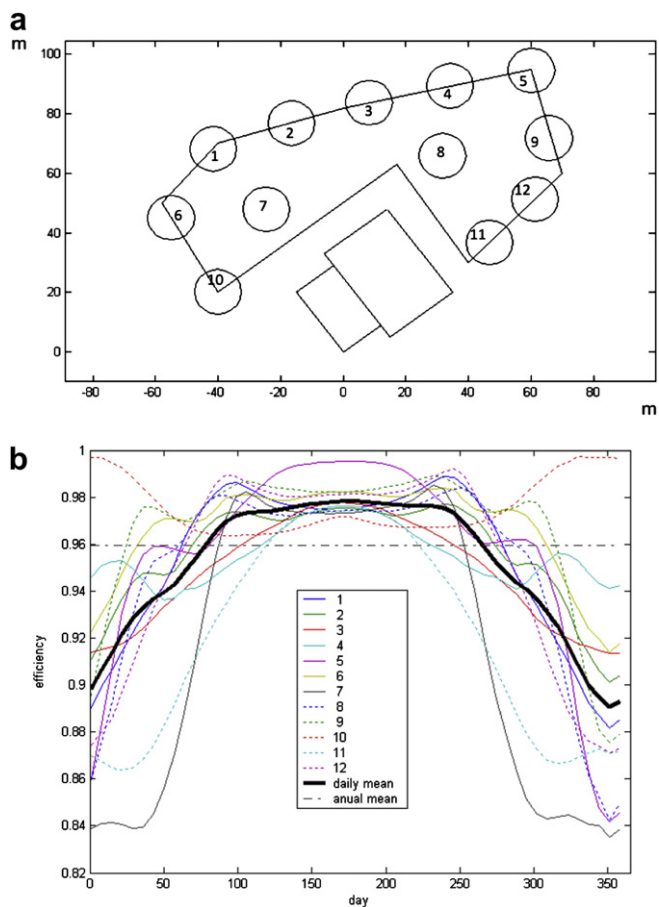


Fig. 30. PV field of 12 PV trackers (a) optimal layout (b) efficiency throughout the year of the PV trackers for the optimal layout.

possible layout of the PV trackers) will be the total electrical energy obtained by all its PV trackers during a mean year:

$$\Psi_S = \sum_{i \in S} W_i - p_i \tag{6}$$

where:

- Ψ_S is the cost function of a population member S .
- W_i is the electrical energy obtained by each PV tracker. The calculus is detailed in Sections 3 and 4.
- p_i is a penalization for populations with PV trackers so close that they cannot complete their turn without colliding amongst

Table 1
Annual efficiency of the 12 PV trackers.

Panel	Efficiency
1	0.962
2	0.961
3	0.954
4	0.957
5	0.965
6	0.971
7	0.931
8	0.959
9	0.972
10	0.973
11	0.930
12	0.961
Average	0.958

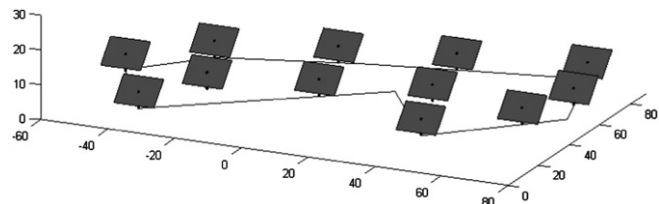


Fig. 31. Best location of the 12 PV trackers in the plot without a house.

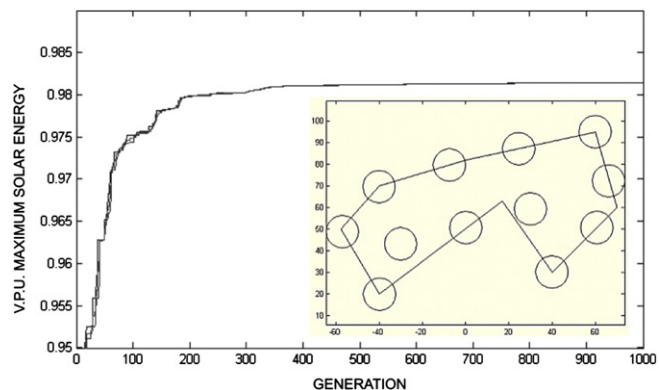


Fig. 32. Evolution of the PV solution efficiency in the plot without a house, and final solution.

themselves. Due to this penalization, the evolution will discard these members of the population.

6. Results

Fig. 24 shows an example of a south oriented plot located at coordinates 41°54'N, 8°52'W. In this figure, the grey area shows the location chosen for an installation consisting of 12 × 9 m² each one. The PV trackers are monocrystalline, efficiency of 130 Wp/m² and utile surface of about 90% of the total area. The total power generated by the installation is 150 kWp and the location has 2260 annual sun hours (51'6% of the solar year hours).

The inverter efficiency of the PV installation is represented in Fig. 25.

Using the celestial mechanical model, the annual solar energy received by a PV tracker, if there aren't cloudy days, is about 3.25 MWh/year.m². The losses caused by clouds in a year for this emplacement are estimated at 25% of the total energy. So, the energy received by a PV tracker would be about 2.44 MWh/year.m². The inverters cannot work with radiations lower than 100 W/m², therefore the annual profitable solar energy is reduced to 2.24 MWh/year.m². Due to the efficiency of PV trackers, about 10%, only

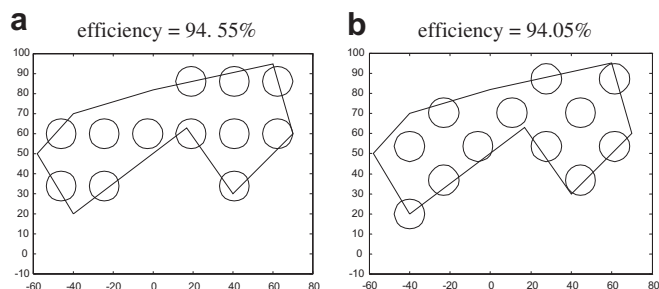


Fig. 33. Field distribution of PV trackers using classical configurations (a) square (b) diagonal.

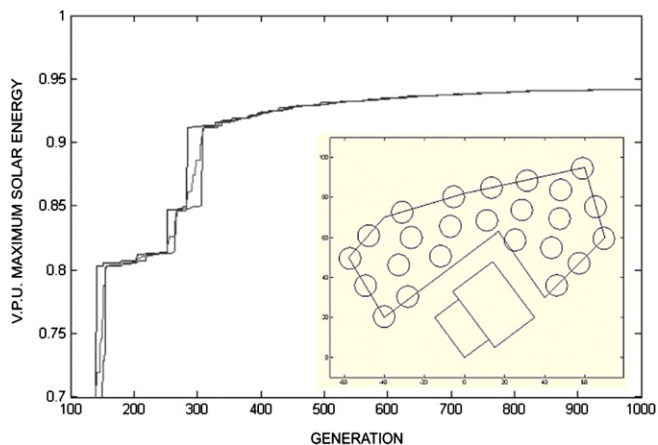


Fig. 34. Evolution of the PV solution efficiency, 24 PV trackers, in the plot with a house, and final solution.

a fraction of the radiation is converted into electrical energy, this is approximately 0.224 MWh/year.m². Therefore, the PV field can generate a maximum electrical energy of 302.3 MWh/year.

Fig. 26 presents the best disposition with the two classical grid configurations: square and diagonal [1]. Above the configurations, their efficiency in percentage of the maximum of electric energy obtainable (302.3 MWh/year) is shown.

These solutions can be improved using the method proposed here. Fig. 27 shows the evolution of the algorithm with an evolutionary strategy ES(3 + 5) during 1000 iterations. It displays the best, the mean and the worst efficiency of each generation. The efficiency achieved is 95.8%. In other words, annual losses caused by shadows are 4.2% of the incoming annual solar energy (approx. 12.7 MWh/m².year). It also presents the final solution, where it can be seen that the PV trackers are far from the house (Fig. 28).

Fig. 29 shows the shadows that have affected the tracker highlighted in black. The shadow percentage produced by its environment is in a grey scale.

Fig. 30 includes the annual efficiency value of each one. The optimal solution implies a total energy of 289.6 MWh/year, and therefore annual losses caused by shadows of 12.7 MWh/year. Table 1 shows the annual efficiency of each of the PV trackers in terms of value per unit of the theoretical maximum electrical energy obtainable (with no shadows).

Figs. 31 and 32 display the results obtained for the above example, if there were no house. In relation to the previous example, the locations of the trackers are now close to the outer perimeter of the plot, and the losses are reduced to less than half, remaining at 1.85%.

Fig. 33 shows the efficiency results achieved by using classical disposition methods. In both cases, results are worse than those achieved with the genetic algorithm.

In the same plot, the photovoltaic facility has been calculated with the same installation power (150 kWp), now installed on 24 PV trackers of 9 × 6 m². Fig. 34 displays the evolution for a ES(5+10). In this case, the annual losses caused by shadows are 5.84%

(equivalent to 17.7 MWh/m².year). As a conclusion, by doubling the number of solar trackers and halving the area of each tracker, less energy is generated. Specifically, losses have increased by 39% compared to the first case calculated in the present section.

7. Conclusions

This paper has introduced an algorithm that allows the calculus of the optimal location of the PV trackers of photovoltaic facility on a building of irregular shape, taking into account the shadows caused by the PV trackers and the obstacles that are on the building or surrounding it, e.g. other buildings, vegetation, etc. Furthermore, a simple method has been presented for the calculus of the shadow suffered by each PV tracker. The percentage of shadow projected onto each tracker is superimposed onto the radiation received data in order to determine the actual radiation that the panel is obtaining. This calculation is carried out for every solar position.

By using the above mentioned method, the efficiency of the PV facility can be increased by 4% with regard to the traditional PV trackers distributions (square or diagonal, Table 2).

Since the metaheuristic and the function cost (shadow calculus algorithms) are loosely coupled, it leaves much room for improvement on the presented results of efficiency, through the use of new and better metaheuristic algorithms.

References

- [1] Meksarik V, Masti S, Taib S, Hadzer CM. Study the effective angle of photovoltaic modules in generating an optimum energy. In: National Power and Energy Conference (PECon), Proceedings; 2003. p. 312–6.
- [2] Chen Yaow-Ming, Wu Hsu-Chin. Determination of the solar cell panel installation angle. In: Proceedings 4th IEEE International Conference on Power Electronics and Drive Systems, vol. 2; 2001. p. 549–54. 2001.
- [3] Chen Yaow-Ming, Lee Chien-Hsing, Wu Hsu-Chin. Calculation of the optimum installation angle for fixed solar-cell panels based on the genetic algorithm and the simulated-annealing method. IEEE Transactions on Energy Conversion June 2005;20(2):467–73.
- [4] Rauschenbach HS. Electrical output of shadowed solar arrays. IEEE Transactions on Electron Devices August 1971;18(8):483–90.
- [5] Weinstock D, Appelbaum J. Shadow variation on photovoltaic collectors in a solar field. In: IEEE Convention of Electrical and Electronics Engineers. Proceedings; Sept. 2004. p. 354–7.
- [6] Ishisaka Y, Harada K, Ishihara Y, Todaka T, Yokouchi H, Yukawa M. Optimization of setting arrays considering the influence of front array's shadow. In: First WCPEC, Proceedings; Dec. 1994. p. 1094–7.
- [7] Quaschnig V, Hanitsch R. Influence of shading on electrical parameters of solar cells. 25th PVSC (IEEE); May 1996:1287–90.
- [8] Fujisawa T, Ohya S. Study on shadow loss of crystalline Si PV module affected by scattering rate of solar irradiance. In: 3rd World Conference on Photovoltaic Energy Conversion; May 2003. p. 1975–6.
- [9] Quaschnig V, Hanitsch R. Irradiance calculation on shaded surfaces. Solar Energy 1998;62(5):369–75.
- [10] Matsukawa H, Shioya M, Kurokawa K. Study on simple assessment method of BIPV power generation for architects. In: Photovoltaic Specialists Conference, Conference Record of the Twenty-Eighth IEEE; Sept. 2000. p. 1648–51.
- [11] Quaschnig V, Hanitsch R. Numerical simulation of current-voltage characteristics of photovoltaic systems with shaded solar cells. Solar Energy 1996; 56(6):513–20.
- [12] Abete A, Barbisio E, Cane F, Demartini P. Analysis of photovoltaic modules with protection diodes in presence of mismatching. In: Twenty First IEEE Photovoltaic Specialists Conference, vol. 2; May 1990. p. 1005–10.
- [13] Karatepe E, Boztepe M, Çolak M. Development of a suitable model for characterizing photovoltaic arrays with shaded solar cells. Solar Energy 2007;81:977–92.
- [14] Karatepe E, Boztepe M, Çolak M. Neural network based solar cell model. Energy Conversion and Management 2006;47:1159–78.
- [15] Woyte A, Nijs J, Belmans R. Partial shadowing of photovoltaic arrays with different system configurations: literature review and field test results. Solar Energy 2003;74:217–33.
- [16] Candela R, Di Dio V, Riva Sanseverino E, Romano P. Reconfiguration techniques of partial shaded PV systems for the maximization of electrical energy production. ICCEP '07. In: International Conference on Clean Electrical Power; May 2007. p. 716–9.
- [17] Winter G, Périaux J, Galan M, Cuesta P. Genetic algorithms in Engineering and Computer Science. New York: Wiley; 1996.

Table 2 Efficiency of the PV facility for different configurations.

No. of trackers	House	Calculus Method		
		Square	Diagonal	Genetic alg.
12	Yes	91.27	91.28	95.80
12	No	94.55	94.05	98.21

- [18] Tom Markvart and Luis Castañer. *Practical Handbook of photovoltaics Fundamentals and applications*. Elsevier Ltd.
- [19] Díaz-Dorado E, Suárez-García A, Carrillo C, Cidrás J. Influence of the shadows in photovoltaic Systems with different configurations of bypass diodes. In: 20th International Symposium on Power Electronics, Electric Drives, Automation and Motion; June 2010.
- [20] Díaz-Dorado E, Suárez-García A, Carrillo C, Cidrás J. Influence of the PV modules layout in power losses of a PV array with shadows. In: 14th International Power Electronics and Motion Control Conference; September 2010.
- [21] Patel Hiren, Agarwal Vivek. MATLAB-Based modeling to study the effects of partial shading on PV array characteristics. *IEEE Transactions on Energy Conversion* March 2008;32:302–10 [Biographies].